S.O.Filin

S.O. Filin *doctor of tech. science*

West Pomeranian University of Technology,
Szczecin 17, al.Piastow, Szczecin, 70-310, Poland,
e-mail: sergiy.filin@zut.edu.pl

CALCULATION OF THE COOLING SPEED OF THE THERMOELECTRIC BEVERAGE COOLER WITH "WET" CONTACT

The paper proposes an engineering technique for calculating beverage cooling speed in a thermoelectric cooler with wet and dry contact. By calculation, the previously proven experimentally conclusion was confirmed that filling the gap between the bottle with the drink and the cooler container can significantly increase the speed of the cooler. The results of comparative calculations are presented by the example of an automobile cooler of drinks Car mini-cooler FM 201.001. The ways of improving the design of the cooler in order to increase its speed are proposed. Bibl. 10, Fig. 5, Tab. 3.

Key words: beverage cooler, cooling speed, heat exchange conditions, thermal resistances.

Introduction

This paper is the second part in a series of three works devoted to the development and research of thermoelectric coolers for drinks with wet contact. In the previous paper [1], the market of modern household and automobile thermoelectric beverage coolers was analyzed in terms of their cooling speed. The performance indicators of these devices do not meet the needs of consumers. Based on the results of experimental studies, the efficiency of the use of the so-called "wet" contact to increase the speed of the coolers was shown. Wet contact is the filling of the air gap between the beverage can or bottle and the cooler container with water or other liquid. The theoretical analysis below allows one to determine the main factors influencing the mentioned efficiency. Another goal of this work is to develop a method for calculating the cooling time of a drink in coolers with wet contact and to compare the results of calculations using the example of data from previous experiments.

Calculation model

Initial data and assumptions

1. As in experiment [1], we take water as a cooled drink which is a liquid with the highest heat capacity. This approach eliminates speculations associated with inaccuracy in determining the thermophysical properties of specific drinks.
2. Similarly, as a container for a drink, we take an aluminum can with a capacity of 0.33 liters. Its parameters are standardized and unified in most countries of the world [4].
3. The parameters of the cooler, including the thermoelectric module, are tied to the actual technical characteristics of coolers of the *Car mini-cooler FM 201.001* type used in the experiment (Fig. 1).

Fig. 1. Car beverage cooler Car mini-cooler ФМ 201.001 (left),
separately to the right - its container with a thermoelectric module installed on it.

4. The bottom of the container in the cooler Car mini-cooler FM 201.001 is made as a separate element of non-metallic material, and the bottom of the can is concave. There is a linear direct contact between the can and the bottom along the circumference of the convex part of the bottom. Therefore, when calculating a dry contact cooler, we assume that the bottom surface does not participate in heat exchange between the container and the beverage can.
5. Due to its smallness, we neglect the thermal resistance of the can. However, in the case of a plastic bottle, this component of the total thermal resistance must be considered.
6. We assume that the space between the container and the cooler body is filled with polyurethane foam insulation (Fig. 2).

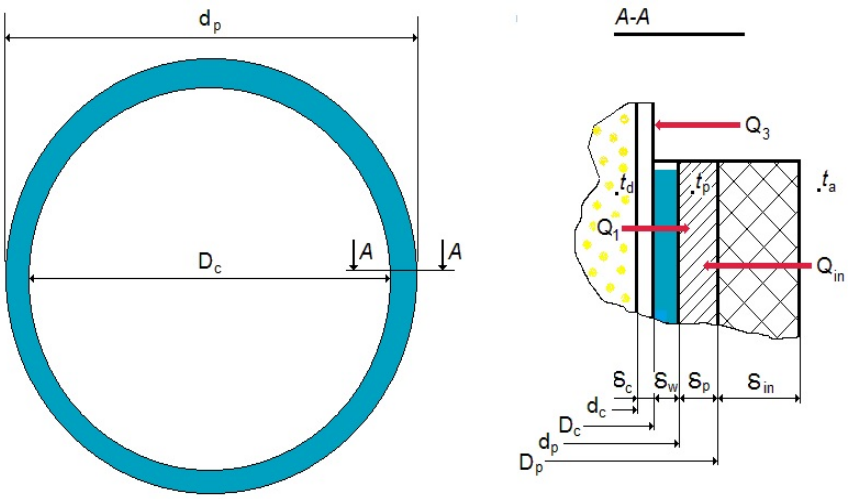

Fig.2. Calculation scheme of beverage cooler.

Table 1

Initial data for the calculation

Parameter	Value	Source	Comment
Cooler capacity			
Material		Manufacturers' data	Aluminum Manganese alloy Al-Mn
Thermal conductivity, λ_p	188 W/m·K	[2]	
Specific mass heat capacity, c_p	985 J/kg K	[2]	
Mass (without bottom part), m_p	113.850 g		Measured
Height, h_p	69 mm		Measured
Inner diameter, d_p	67 mm		Measured
Thickness, δ_p	2 mm		Measured
Water in container			
Thermal conductivity, λ_w	0.55 W/m·K	[3]	At a temperature of 10°C
Specific mass heat capacity, c_w	4200 J/kg·K	[3]	At a temperature of 10°C
Total mass, m_w	15.0 g		Measured
Including mass of water mass in a cylindrical gap, m_{w1}	7.1 g		Calculated
Height, h_w	68 mm		1 mm less than h_p
Layer thickness, δ_w	0.5 mm		$(d_p - D_c)/2$
Beverage can			
Material		[4]	Aluminum alloy АМг2
Thermal conductivity, λ_c	159 W/m·K	[5]	
Specific mass heat capacity, c_c	963 J/kg·K	[5]	
Mass, m_c	13.280 g		Measured
Outer diameter, D_c	66 mm	[4]	
Height, h_c	115.2 mm	[4]	
Thickness, δ_c	0.11...0.30 mm	[4]	0.11 – in the cylindrical part 0.30 – in the lower part
Beverage (water)			
Thermal conductivity, λ_d	0.574 W/m·K	[3]	At a temperature of 15°C[1]
Specific mass heat capacity, c_d	4190 J/kg·K	[3]	At a temperature of 15°C
Mass, m_d	332.0 g		Measured
Insulation			
Material			Foamed polyurethane
Thermal conductivity, λ_{in}	0.029 W/m·K	[6]	
Specific heat capacity, c_{in}	1.47	[6]	
Density, σ_{in}	40 kg/m^3	[6],[7]	
Thickness, δ_{in}	6.5 mm		Measured

[1] Taken as the average temperature of the beverage in the process of cooling.

Calculation of theoretically minimum cooling time

The minimum time τ_{min} for cooling a beverage in a can to a temperature t_f (under ideal conditions of heat exchange at the boundaries of media) can be found from the heat balance of the cold side of the cooler:

$$\left(\bar{Q}_0 - \bar{Q}_2 - \bar{Q}_3 - \bar{Q}_{in}\right)\cdot\tau_{\min} = \bar{Q}_d + \bar{Q}_c + \bar{Q}_w + \bar{Q}_p + \bar{Q}_{in} \quad (1)$$

$$\left(\bar{Q}_0 - \bar{Q}_2 - \bar{Q}_3 - \bar{Q}_{in}\right)\cdot\tau_{\min} =$$

$$= m_d c_d \cdot\left(t_a - t_f\right) + \left(m_w c_w + m_c c_c + m_p c_p\right)\cdot\left(t_a - t_p\right) + \left(m_{in} c_{in}\right)\cdot\frac{t_a - t_p}{2} \quad (2)$$

where: $\bar{Q}_0$ is average cooling capacity of thermoelectric module during cooling; $\bar{Q}_2$ is average heat input from the environment through the bottom of the can, $\bar{Q}_3$ is average power of heat input from the environment to the upper part of the can, not immersed in the container, $\bar{Q}_{in}$ is average power of heat input from the environment through the insulation, Q_d, Q_c, Q_w, Q_p, Q_{in} is the amount of heat removed from the drink, can, water in the gap, container and insulation, respectively, m is mass, c is heat capacity, t_a is air temperature in the room and the initial temperature of all the elements, t_f is finish temperature of the beverage, t_p is average temperature of the cooler at the end of cooling process.

The only unknown value in Eq.(2) is temperature t_p. One can calculate it from the thermal balance of the gap or use the experimental data. Putting into calculation the values $t_a = 25$ °C, $t_f = 10$ °C, $t_p = 8.2$ °C and substituting data from Table 1, we obtain:

Table 2

Intermediate results of calculating thermal balance components

Object	Designation	$m_i c_i$ [J/K]	Q_i, [J]	Percentage
Beverage	$m_d c_d$, Q_d	1382.7	20740.5	87.44%
Can	$m_c c_c$, Q_c	11.95	200.76	0.85%
Water in the gap	$m_w c_w$, Q_w	62.85	1055.88	4.45%
Container	$m_p c_p$, Q_p	102.46	1721.3	7.26%
Insulation	$m_{in} c_{in}$, Q_{in}	0.013	0.1065	0.0005%
Sum	**Σ**	**1560**	**23718.6**	**100%**

It follows from the presented data that, in terms of mass heat capacity, the presence of water in the gap increases the thermal load on the module by less than 5%. The influence of the can (0.85%) is within the experimental error, and therefore, may not be taken into account in engineering calculations, similarly to the effect of insulation, which is absolutely negligible. The role of thermal resistances of the same elements is analyzed below. A similar conclusion in relation to insulation can be made when analyzing the structure of heat inputs. In [9], [10] it was shown that the isolation of the ice form of thermoelectric ice

cube ice makers does not increase the ice maker productivity, because the lion's share of the heat load is the process of the water-ice phase transition. Despite the fact that in our example we are not talking about freezing a beverage, the contribution of heat inputs from the environment is also not vital. Both in the case of ice makers and in coolers, i.e. in the products where the dynamic characteristics are decisive, the thermal resistance of the layers of materials between the cooled object and the source of cold has a greater influence than the mass heat capacity. This thesis is confirmed by the experimental data and further calculations.

Algorithm for calculating the average cooling capacity of the module $\bar{Q}_0$

To be able to use the module manufacturers' data given in Table 3 and in Fig. 3, it is worthwhile to:

1) interpolate the values Q_{omax} and ΔT_{max} between the two temperatures of the hot side of the cooler (the manufacturer provides data for temperatures 27 and 50 °C) for the temperature t_h of the hot heat sink in the steady state, which was measured during the experiment, i.e. for t_h = 32 °C;

2) determine the value of relative current I/I_{max}. In our case it is 2.15/3.4 = 0.63;

3) build dependence Q_{omax} (ΔT_{max}) for this ratio and the above temperature t_h;

4) using the above assumptions, calculate $\Delta T = t_h - t_p$ and graphically determine $\bar{Q}_0$ as shown in Fig. 4.

Another possible option is calculation of $\bar{Q}_0$ by the formula proposed in [8].

Table 3

Technical parameters of module MT-1-1.45-143S

Parameters	**Unit**	**MT 1-1.45-143S**
Current, max	A	3.4
Voltage, max	V	16.6
Coolling Pover, max, (at Th=27°C)	W	33
Temp. Difference, max, (at T_h=27°C in vacuum)	K	70
Resistance (at T_h=27°C amb)	Ohm	4.56 ± 10 %
Width	mm	40+0.5/-0.1
Length	mm	40+0.5/-0.1
Thickness	mm	3.8
Thickness tolerance	mm	±0.3
Parallel Difference	mm	0.05
Wire Length	mm	120+10
Wire Section	mm^2	0.035
Operating temperature, max	°C	90

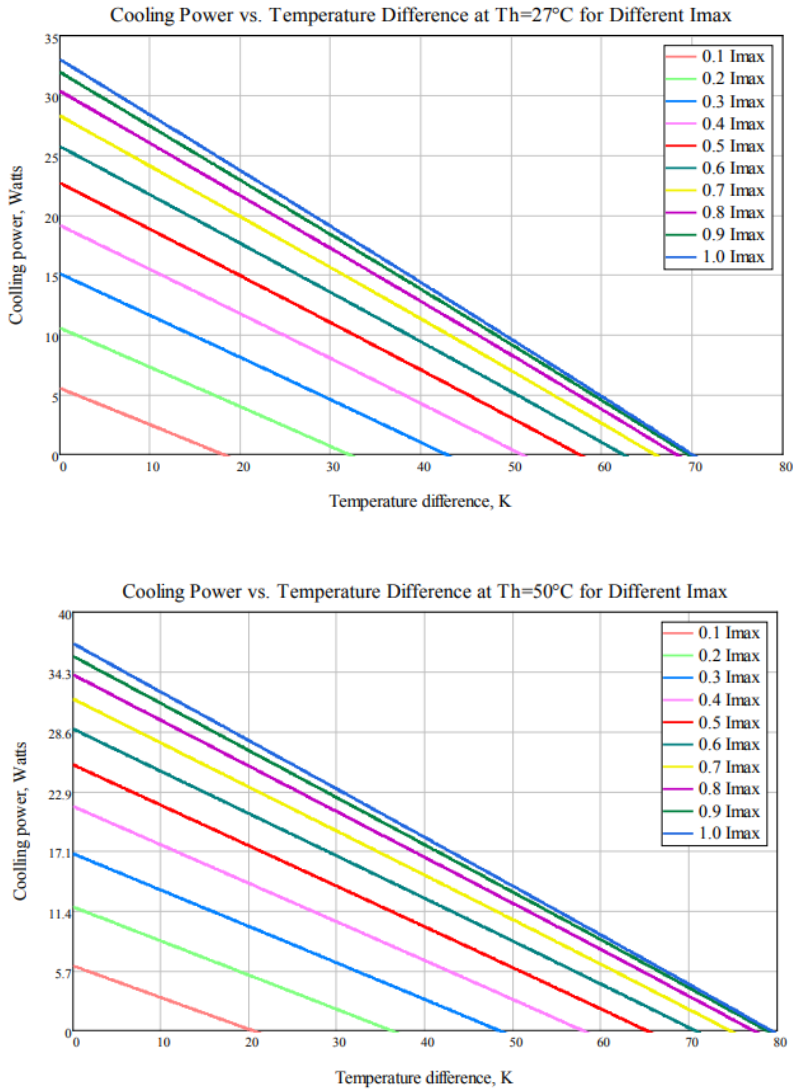

Fig.3. Load characteristics of module MT-1-1.45-143S.

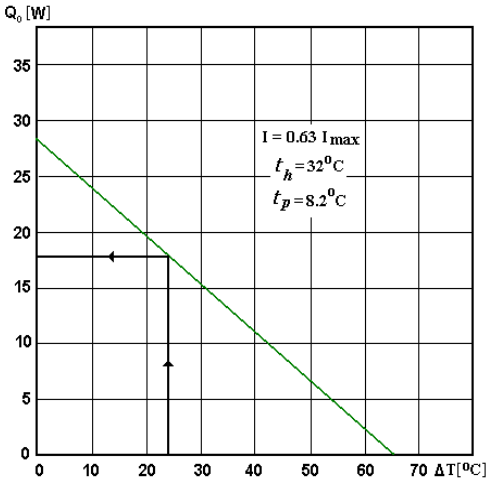

Fig. 4. Graphical method for determining the cooling capacity of the MT-1-1.45-143S module under steady state operation on the manufacturers' database (Fig. 3).

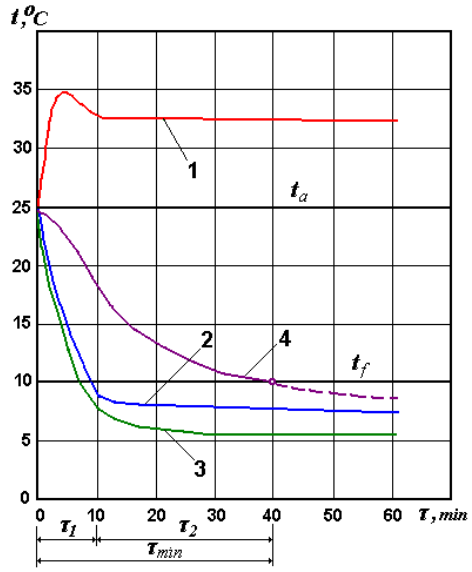

Fig.5. Typical dynamics of temperature change on the cold and hot side of module of thermoelectric cooler at ambient temperature t_a = 25°C:
1 – hot heat sink temperature t_h, 2 – container temperature at wet contact t_{pw},
3 – container temperature at dry contact t_{pd}, 4 – average beverage temperature t_d.

Due to the variability of temperatures on both sides of the thermoelectric module, the value $\bar{Q}_0$ is also not constant. Its relative stabilization occurs approximately 10 minutes after the cooler is turned on (Fig. 5). Therefore, in order to increase the calculation accuracy, one can separately determine the values of Q_{01}, and Q_{02} for two time intervals τ_1 и τ_2 and then use the formula (3)

$$\bar{Q}_0 = \frac{Q_{01} \cdot \tau_1 + Q_{02} \cdot (\tau_{\min} - \tau_1)}{\tau_{\min}} \quad , \tag{3}$$

where τ_1 = 10 minutes.

On substituting (3) into (2) we find τ_{min}.

$$\tau_{\min} = (\frac{\sum Q_i - 10 \cdot 60 \cdot Q_{01}}{Q_{02}}) + 10 \cdot 60 = 1244.9s = 20m48s \quad , \tag{4}$$

where Q_{01} = 20.4 W, Q_{02} = 17.8 W.

The calculation of values $\bar{Q}_2$, $\bar{Q}_3$, $\bar{Q}_{in}$ by the known dependences for heat transfer through a multi-layer wall and for natural convection in air (with regard to the data in Table 4) yielded the following results: $\bar{Q}_2$ = 0.027 W, $\bar{Q}_3$ = 0.063 W, $\bar{Q}_{in}$ = 0.019 W. The sum of these three heat inputs (0.109 W) is as little as 0.6% of the average cooling capacity of module, which makes it possible to ignore them in the engineering calculations.

Actual time of beverage cooling from 25 °C to 10 °C is a factor of 2.5 longer (Table 5), which is due to thermal resistances of layers δ_c , δ_w and δ_p (Fig.2).

Calculation of cooling time with regard to thermal resistances of layers

To take into account the influence of the thermal resistance of the media layers located in the gap between the beverage and the cold source (module), it is necessary to use the thermal balance of the cooled object in a regular thermal mode [3,11]:

$$\sum(m_i c_i)\cdot d(\Delta t_1) = k_\Sigma \cdot F \cdot \Delta t_f \cdot d(\tau) \tag{5}$$

Solving Eq.(5) for τ, we obtain:

$$\tau = \frac{\sum m_i c_i}{k_\Sigma F} \ln \frac{t_a - t_p}{t_f - t_p} \quad , \tag{6}$$

where:

$$k_\Sigma = \frac{1}{\frac{1}{\alpha_d} + \frac{\delta_w}{\lambda_w} + \frac{\delta_p^*}{\lambda_p}} \quad . \tag{7}$$

In relation (6), we separately take into account the heat exchange through the container bottom made of rigid plastic (λ_b = 0.2 W/mK). In relation (7), in the calculation of the container thermal resistance δ_p^*/λ_p, we use the reduced thickness δ^*_p, calculated by formula (8):

$$\delta_p^* = \frac{F_1\delta_1 + (F - F_1)\delta_2}{F} \quad , \tag{8}$$

where: $F_1 = h_p a_m$, $F = \pi d_p h_p$, $\delta_1 = \delta_p + 5\ mm$ (see Fig.1), $\delta_2 = ½(½\pi d_p - a_m/2)$.

Substituting the data from Table 1 and assuming the coefficient of heat transfer from water to the can wall α_d = 140 W/m^{2}K [12,13], we obtain δ^*_p = 36 mm, k_Σ = 122.1 W/m^{2}K.

Conclusions

A laboratory for remote monitoring and control of the heat generation unit operation has been developed. The established laboratory provides an opportunity to study the methods of backup power management due to electricity generated by an array of solar panels located outside the room with the heat generation unit and thermoelectric elements mounted thereupon. **The scientific novelty** of the results obtained lies in the fact that the methods of combining various processes of energy generation from one source and methods of emergency power supply for the control elements of this process have been further developed. **The practical significance** of the results obtained is that the created lab allows holding experiments with different cases of regular stopping of heat generation process in case of unstable or missing power supply for control units. **Prospects for further research** are to develop methods of regular shutdown of the heat generation unit in conditions, when the elements of control and monitoring of the unit are not provided with regular power supply.

The work was supported by the grant of State Fundamental Research Foundation according to contract Ф83-111/2018.

References

1. Deasy, M.J., et al. (2018). Electricity generation from a biomass cookstove with MPPT power

management and passive liquid cooling. *Energy for Sustainable Development*, 43, 162–172, doi:10.1016/j.esd.2018.01.004.
2. Gopi, Nikhil Pattath, and Subhakar Devendran (2015). Autonomy considerations for a standalone photovoltaic system. *Sustainable Energy Technologies and Assessments*, 10, 79–83., doi:10.1016/j.seta.2015.03.005.
3. Eldesoukey, Ayman, and Hamdy Hassan (2019). 3D model of thermoelectric generator (TEG) case study: effect of flow regime on the TEG performance. *Energy Conversion and Management*, 180, 231–239, doi:10.1016/j.enconman.2018.10.104.
4. Yang, Haoqi, et al. (2018). Optimization of thermoelectric generator (TEG) integrated with three-way catalytic converter (TWC) for harvesting engine's exhaust waste heat. *Applied Thermal Engineering*, 144, 628–638, doi:10.1016/j.applthermaleng.2018.07.091.
5. Kütt, Lauri, et al. (2018). Thermoelectric applications for energy harvesting in domestic applications and micro-production units. Part I: Thermoelectric concepts, domestic boilers and biomass stoves. *Renewable and Sustainable Energy Reviews*, 98, 519–544, doi:10.1016/j.rser.2017.03.051.
6. Sornek, Krzysztof, et al. (2019). Comparative analysis of selected thermoelectric generators operating with wood-fired stove. *Energy*, 166, 1303–1313., doi:10.1016/j.energy.2018.10.140.
7. Nuwayhid, Rida Y., et al. (2005). Development and testing of a domestic woodstove thermoelectric generator with natural convection cooling. *Energy Conversion and Management*, 46(9-10), 1631–1643, doi:10.1016/j.enconman.2004.07.006.
8. Zhao, Yulong, et al. (2018). Performance analysis of automobile exhaust thermoelectric generator system with media fluid, *Energy Conversion and Management,* 171, 427–437, doi:10.1016/j.enconman.2018.06.006
9. Champier, Daniel. (2017).Thermoelectric generators: a review of applications. *Energy Conversion and Management,* 140, 167–181, doi:10.1016/j.enconman.2017.02.070.
10. Price-Allison, A., et al. (2019). Emissions performance of high moisture wood fuels burned in a residential stove. *Fuel*, 239, 1038–1045, doi:10.1016/j.fuel.201810.1016/j.fuel.2018.11.090.

Submitted 13.05.2020

Філін С.О. *доктор техн. наук*

Західнопоморський технологічний університет в Щецині
алея Піаст, 17, Щецін, 70-310, Польща,
e-mail: sergiy.filin@zut.edu.pl

РОЗРАХУНОК ШВИДКОДІЇ ТЕРМОЕЛЕКТРИЧНОГО ОХОЛОДЖУВАЧА НАПОЇВ З «МОКРИМИ» КОНТАКТОМ

У статті запропоновано інженерну методику розрахунку швидкості охолодження напою в термоелектричному охолоджувачі з мокрим і сухим контактом. Розрахунковим шляхом був підтверджений раніше доведений експериментально висновок про те, що заповнення щілини між пляшкою з напоєм і ємністю охолоджувача дозволяє істотно підвищити швидкодію охолоджувача. Представлено результати порівняльних розрахунків на прикладі автомобільного

охолоджувача напоїв Car mini-cooler FM 201.001. Запропоновано шляхи удосконалення конструкції охолоджувача з метою підвищення його швидкодії. Бібл. 10, рис. 5, табл. 3.
Ключові слова: охолоджувач напоїв, швидкість охолодження, умови теплообміну, теплові опори.

Филин С.О. *доктор техн. наук*

Западнопоморский технологический университет в Щецине
аллея Пиастов, 17, Щецин, 70-310, Польша,
e-mail: sergiy.filin@zut.edu.pl

РАСЧЁТ БЫСТРОДЕЙСТВИЯ ТЕРМОЭЛЕКТРИЧЕСКОГО ОХЛАДИТЕЛЯ НАПИТКОВ С «МОКРЫМ» КОНТАКТОМ

В статье предложнена инженерная методика рассчёта скорости охлаждения напитка в термоэлектрическом охладителе с «мокрым» и «сухим» контактами. Расчётным путём был подтверждён ранее доказанный экспериментально вывод о том, что заполнение щели между бутылкой с напитком и ёмкостью охладителя позволяет существенно повысить быстродействие охладителя. Представлены результаты сравнительных расчётов на примере автомобильного охладителя напитков Car mini-cooler ФМ 201.001. Предложены пути усовершенствования конструкции охладителя с целью повышения его быстродействия. Библ. 10, рис. 5, табл. 3.
Ключевые слова: охладитель напитков, скорость охлаждения, условия теплообмена, тепловые сопротивления.

References

1. Deasy, M.J., et al. (2018). Electricity generation from a biomass cookstove with MPPT power management and passive liquid cooling. *Energy for Sustainable Development*, 43, 162–172, doi:10.1016/j.esd.2018.01.004.
2. Gopi, Nikhil Pattath, and Subhakar Devendran (2015). Autonomy considerations for a standalone photovoltaic system. *Sustainable Energy Technologies and Assessments*, 10, 79–83., doi:10.1016/j.seta.2015.03.005.
3. Eldesoukey, Ayman, and Hamdy Hassan (2019). 3D model of thermoelectric generator (TEG) case study: effect of flow regime on the TEG performance. *Energy Conversion and Management*, 180, 231–239, doi:10.1016/j.enconman.2018.10.104.
4. Yang, Haoqi, et al. (2018). Optimization of thermoelectric generator (TEG) integrated with three-way catalytic converter (TWC) for harvesting engine's exhaust waste heat. *Applied Thermal Engineering*, 144, 628–638, doi:10.1016/j.applthermaleng.2018.07.091.
5. Kütt, Lauri, et al. (2018). Thermoelectric applications for energy harvesting in domestic applications and micro-production units. Part I: Thermoelectric concepts, domestic boilers and biomass stoves. *Renewable and Sustainable Energy Reviews*, 98, 519–544, doi:10.1016/j.rser.2017.03.051.
6. Sornek, Krzysztof, et al. (2019). Comparative analysis of selected thermoelectric generators operating with wood-fired stove. *Energy*, 166, 1303–1313., doi:10.1016/j.energy.2018.10.140.

7. Nuwayhid, Rida Y., et al. (2005). Development and testing of a domestic woodstove thermoelectric generator with natural convection cooling. *Energy Conversion and Management*, 46(9-10), 1631–1643, doi:10.1016/j.enconman.2004.07.006.
8. Zhao, Yulong, et al. (2018). Performance analysis of automobile exhaust thermoelectric generator system with media fluid, *Energy Conversion and Management,* 171, 427–437, doi: 10.1016/j.enconman.2018.06.006
9. Champier, Daniel. (2017).Thermoelectric generators: a review of applications. *Energy Conversion and Management,* 140, 167–181, doi:10.1016/j.enconman.2017.02.070.
10. Price-Allison, A., et al. (2019). Emissions performance of high moisture wood fuels burned in a residential stove. *Fuel*, 239, 1038–1045, doi:10.1016/j.fuel.201810.1016/j.fuel.2018.11.090.

Submitted 13.05.2020